J. Fluid Mech. (1993), *vol.* 249, *pp.* 441–463

Inviscid instability of a skewed compressible mixing layer

By GANYU LU AND SANJIVA K. LELE†
Department of Mechanical Engineering, Stanford University, Stanford, CA 94305, USA

(Received 27 April 1992 and in revised form 26 October 1992)

In this paper we study the inviscid instability of a skewed compressible mixing layer between streams of different velocity magnitude and direction. The mean flow is governed by the three-dimensional laminar boundary-layer equations and can be reduced to a sum of a uniform flow and a two-dimensional shear flow. In the stability analysis, the amplification direction is assumed to be normal to the homogeneous direction of the mean flow. The results show that skewing enhances the instability by a factor of three for the incompressible mixing layer with velocity ratio 0.5 and uniform temperature. Under compressible conditions, skewing still increases the maximum amplification rate for a medium convective Mach number, but the enhancement is smaller. A scaling of the skewing effect is introduced which quantitatively explains the linear stability behaviour. Similarly, a suitably defined convective Mach number explains the compressibility effect.

1. Introduction

There are numerous aerodynamic situations in which a mixing layer is three-dimensional instead of being the frequently studied idealization of a two-dimensional one. For example, the initial spreading of a swirling jet involves a three-dimensional mixing layer. It occurs over the surface of a jet plume issuing from a surface into a mainstream. The vortex sheet rolling up from a slender delta wing at incidence and most three-dimensional boundary-layer separations involve complex mixing layers. In many practical flows, the effects of pressure gradients, flow curvature and three-dimensional mean flow occur simultaneously, making it difficult to interpret the individual effects. In this paper, we isolate the skewing effect and examine the inviscid instability of the skewed compressible mixing layer, which forms between two streams with different directions, velocity magnitudes and temperatures.

Both experimental (e.g. Brown & Roshko 1974; Papamoschou & Roshko 1988) and computational (e.g. Ragab & Wu 1988; Lele 1989; Sandham & Reynolds 1989; Jackson & Grosch 1989) studies show that flow stability increases at high convective Mach numbers. If a mixing-layer configuration is used to mix fuel and oxidizer, this increased stability may result in poor mixing leading to partial burning and decreased combustion efficiency. For a supersonic combustion application, good mixing is essential to a feasible design. Skewing the two streams may enhance the mixing. To date, experiments regarding this flow are very limited. Hackett & Cox (1970) conducted experiments on the turbulent mixing between two grazing perpendicular streams. Unfortunately their experiments were restricted to only one value of the skewing angle,

† Also with the Department of Aeronautics and Astronautics, Stanford University.

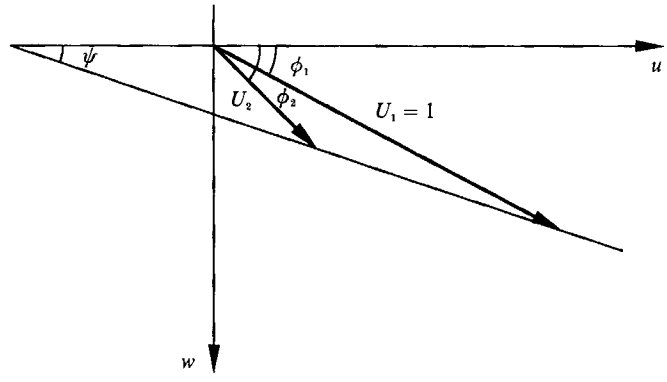

FIGURE 1. Top view of velocity vector (u, w) for a skewed mixing layer.

namely 90°, and they compared this skewed mixing layer with a plane mixing layer with zero velocity ratio. In such a comparison the effects of skewing and different velocity ratio occur together. The present work isolates the skewing effect from the effects of velocity ratio, density ratio and flow compressibility. Our results of the skewing effect on incompressible mixing layers agree very well with the experimental results of Hackett & Cox. Another experimental study has been initiated recently by Gründel & Fiedler (1992). Flow visualizations and preliminary measurements in a mixing layer with equal but oppositely skewed free streams have been reported. This configuration is similar to that used by Hackett & Cox but with a different skewing angle, namely 30°, and vortex generators at the trailing edge are used to disturb the mixing layer. Helical vortex structures which exhibit a spanwise merger have been reported.

The instability of a skewed compressible mixing layer has not been studied in detail, one exception being a recent study by Grosch & Jackson (1991). They formulated the mean flow equations and performed linear stability analysis on idealized mean flow profiles. They also assumed that the amplification direction of the instability waves is the same as the propagation direction. Macaraeg (1991) has extended the analysis of Grosch & Jackson to consider bounded free shear flows and has also performed numerical simulations for the temporal problem. In this paper we consider a different situation: the instability growth in a skewed mixing layer possessing a homogeneous direction. The mixing layer downstream of a splitter plate is homogeneous in the direction of the splitter plate edge. When the splitter plate edge receptivity is dominant, the spatial amplification of instability waves occurs in the direction normal to the imposed homogeneous coordinate.

To identify the skewing effect, the maximum spatial amplification rate of the skewed mixing layer is compared with that of the corresponding unskewed mixing layer. The exact effect of skewing is compared with a geometrically derived scaling of the skewing effect. This comparison shows that skewing has the simultaneous effect of increasing the effective velocity ratio, which is a destabilizing effect, and increasing the effective convective Mach number, which is a stabilizing effect. For the incompressible mixing layer with velocity ratio 0.5 and uniform temperature, skewing enhances the instability growth rate by a factor of three. Under compressible conditions this enhancement is moderate with the effect decreasing with increasing convective Mach number.

In §2 the three-dimensional boundary-layer equations are solved and reduced to a sum of a uniform flow and a two-dimensional shear flow. Section 3 contains inviscid compressible stability equations and some relations of the wavenumbers and

frequencies of the skewed mixing layer and its equivalent two-dimensional flow. Section 4 gives the numerical results showing the effects of skewing and compressibility. Scaling which isolates the skewing effect is also presented in this section. Section 5 follows with further discussion and the final section presents our conclusions.

2. Mean flow

We consider a skewed compressible mixing layer, which separates two streams of different velocity magnitudes and directions and different temperatures. We choose the y-coordinate normal to the layer, and assume that there is a homogeneous direction chosen as the z-coordinate so that $\partial/\partial z = 0$ for the mean flow. The pressure gradient is assumed to be zero and the fluid is a perfect gas with constant specific heats. The mean flow is governed by the three-dimensional compressible boundary-layer equations

$$\frac{\partial \rho u}{\partial x} + \frac{\partial \rho v}{\partial y} = 0, \tag{2.1a}$$

$$\rho u \frac{\partial u}{\partial x} + \rho v \frac{\partial u}{\partial y} = \frac{1}{Re} \frac{\partial}{\partial y}\left(\mu \frac{\partial u}{\partial y}\right), \tag{2.1b}$$

$$\rho u \frac{\partial w}{\partial x} + \rho v \frac{\partial w}{\partial y} = \frac{1}{Re} \frac{\partial}{\partial y}\left(\mu \frac{\partial w}{\partial y}\right), \tag{2.1c}$$

$$\rho u \frac{\partial T}{\partial x} + \rho v \frac{\partial T}{\partial y} = \frac{1}{Re\,Pr} \frac{\partial}{\partial y}\left(\mu \frac{\partial T}{\partial y}\right) + \frac{M^2(\gamma-1)}{Re} \mu \left[\left(\frac{\partial u}{\partial y}\right)^2 + \left(\frac{\partial w}{\partial y}\right)^2\right], \tag{2.1d}$$

$$\rho T = 1, \tag{2.1e}$$

where all the variables are non-dimensionalized using the magnitudes of the fast-moving free stream, and the reference lengthscale is, for the time being, an arbitrary constant. A suitable choice of the lengthscale will be made later. In the above equations (u, v, w) are the velocity components in the (x, y, z)-directions, ρ the density, T the temperature.The dynamic viscosity μ is assumed to be only a function of temperature. The ratio of specific heats γ and the Prandtl number Pr are assumed to be constant, and the Mach number M and the Reynolds number Re are defined using the fast-moving-stream reference values. The boundary conditions are

$$u(+\infty) = \cos\phi_1, \quad u(-\infty) = U_2 \cos\phi_2, \tag{2.2a}$$

$$w(+\infty) = \sin\phi_1, \quad w(-\infty) = U_2 \sin\phi_2, \tag{2.2b}$$

$$T(+\infty) = 1, \quad T(-\infty) = T_2, \tag{2.2c}$$

where U_2 is the velocity ratio and is assumed, without loss of generality, to be not larger than unity, and T_2 is the temperature ratio. As shown in figure 1, the skewing angles of the high- and low-speed streams measured clockwise from the x-axis are ϕ_1 and ϕ_2, respectively, and

$$\phi \equiv \phi_2 - \phi_1 \tag{2.3}$$

is the relative skewing angle of the slow stream with respect to the fast stream.

We introduce the Howarth transformation (Schlichting 1979)

$$Y = \int_0^y \rho \, dy, \quad V = \rho v + u \int_0^y \frac{\partial \rho}{\partial x} dy \tag{2.4}$$

to transform the mean flow equations into the incompressible form

$$\frac{\partial u}{\partial x}+\frac{\partial V}{\partial Y}=0, \tag{2.5a}$$

$$u\frac{\partial u}{\partial x}+V\frac{\partial u}{\partial Y}=\frac{1}{Re}\frac{\partial}{\partial Y}\left(\frac{\mu}{T}\frac{\partial u}{\partial Y}\right), \tag{2.5b}$$

$$u\frac{\partial w}{\partial x}+V\frac{\partial w}{\partial Y}=\frac{1}{Re}\frac{\partial}{\partial Y}\left(\frac{\mu}{T}\frac{\partial w}{\partial Y}\right), \tag{2.5c}$$

$$u\frac{\partial T}{\partial x}+V\frac{\partial T}{\partial Y}=\frac{1}{Re\,Pr}\frac{\partial}{\partial Y}\left(\frac{\mu}{T}\frac{\partial T}{\partial Y}\right)+\frac{M^2(\gamma-1)}{Re}\frac{\mu}{T}\left[\left(\frac{\partial u}{\partial Y}\right)^2+\left(\frac{\partial w}{\partial Y}\right)^2\right], \tag{2.5d}$$

$$\rho T=1. \tag{2.5e}$$

We then seek similarity solutions in terms of

$$\eta = Y(Re/x)^{\frac{1}{2}} \tag{2.6}$$

and of the form

$$u=f'(\eta), \quad V=\frac{1}{2(Re\,x)^{\frac{1}{2}}}(\eta f'-f), \quad w=g(\eta), \quad T=h(\eta). \tag{2.7}$$

Substituting (2.7) into (2.5) and assuming that viscosity is a linear function of temperature, we obtain

$$2f'''+ff''=0, \tag{2.8a}$$

$$2g''+fg'=0, \tag{2.8b}$$

$$\frac{2}{Pr}h''+fh'=-2M^2(\gamma-1)(f''^2+g'^2). \tag{2.8c}$$

Equation (2.8*a*) is decoupled from (2.8*b*) and (2.8*c*) and can be solved for f. Equations (2.8*b*) and (2.8*c*) suggest solutions of the form

$$g=g(u), \quad h=h(u). \tag{2.9}$$

Substituting (2.9) into (2.8*b*) and using the boundary conditions (2.2) yields

$$w=u\tan\psi+\frac{U_2\sin\phi}{\cos\phi_1-U_2\cos\phi_2}, \tag{2.10}$$

where

$$\tan\psi=\frac{\sin\phi_1-U_2\sin\phi_2}{\cos\phi_1-U_2\cos\phi_2}. \tag{2.11}$$

Note that the (x, z) projection of the velocity vector (u, w) lies on a straight line with an angle ψ from the x-axis. This geometric property of the similarity solution is shown in figure 1. It is convenient to re-express the velocity (u, w), where w is given by (2.10), as

$$u=\tilde{u}\cos\psi+U_0, \quad w=\tilde{u}\sin\psi+W_0, \tag{2.12}$$

where

$$W_0=U_0\tan\psi+\frac{U_2\sin\phi}{\cos\phi_1-U_2\cos\phi_2}, \tag{2.13}$$

and $\tilde{u}=\tilde{f}'(\eta)$ is given by

$$2\tilde{f}'''+\tilde{f}\tilde{f}''\cos\psi+U_0\eta\tilde{f}''=0. \tag{2.14}$$

If we choose U_0 and W_0 such that

$$U_0=\cos\phi_1-\cos\psi, \quad W_0=\sin\phi_1-\sin\psi, \tag{2.15}$$

then the boundary conditions for $\tilde{u}$ become

$$\tilde{u}(+\infty) = 1, \quad \tilde{u}(-\infty) = \tilde{U}_2 = 1-(1-2U_2\cos\phi+U_2^2)^{\frac{1}{2}}. \tag{2.16}$$

The vorticity thickness for the two-dimensional mixing layer can be defined as

$$\delta_\omega^* = \frac{1-\tilde{U}_2}{|\mathrm{d}\tilde{u}/\mathrm{d}y^*|_{\max}}, \tag{2.17}$$

where the asterisk represents dimensional variables. Similarly, for the skewed mixing layer, we may define vorticity thickness for the u and w velocity components as (for $\phi_1 \neq 0$ or $\phi_2 \neq 0$)

$$\delta_{\omega_u}^* = \frac{\cos\phi_1 - U_2\cos\phi_2}{|\mathrm{d}u/\mathrm{d}y^*|_{\max}}, \quad \delta_{\omega_w}^* = \frac{\sin\phi_1 - U_2\sin\phi_2}{|\mathrm{d}w/\mathrm{d}y^*|_{\max}}. \tag{2.18}$$

Since u, w, and $\tilde{u}$ have linear relations, we have

$$\delta_\omega^* = \delta_{\omega_u}^* = \delta_{\omega_w}^*, \tag{2.19}$$

which is chosen as the characteristic lengthscale from here on in this paper.

The 'momentum' thickness for the two-dimensional mixing layer is also often used and is defined as

$$\delta_m^* = \frac{1}{(1-\tilde{U}_2)^2}\int_{-\infty}^{+\infty}(1-\tilde{u})(\tilde{u}-\tilde{U}_2)\,\mathrm{d}y^*. \tag{2.20}$$

A similar definition of the momentum thickness for the skewed mixing layer is

$$\delta_{m_u}^* = \frac{1}{(\cos\phi_1 - U_2\cos\phi_2)^2}\int_{-\infty}^{+\infty}(\cos\phi_1 - u)(u - U_2\cos\phi_2)\,\mathrm{d}y^*, \tag{2.21a}$$

$$\delta_{m_w}^* = \frac{1}{(\sin\phi_1 - U_2\sin\phi_2)^2}\int_{-\infty}^{+\infty}(\sin\phi_1 - w)(w - U_2\sin\phi_2)\,\mathrm{d}y^*, \tag{2.21b}$$

which also satisfies

$$\delta_m^* = \delta_{m_u}^* + \delta_{m_w}^*. \tag{2.22}$$

If the Prandtl number is assumed to be unity, substituting (2.9) and (2.10) into (2.8c) yields an equivalent Crocco–Busemann relation

$$T = \frac{M^2(\gamma-1)}{2\cos^2\psi}[(\cos\phi_1 + U_2\cos\phi_2)u - u^2 - U_2\cos\phi_1\cos\phi_2] + \frac{T_2(\cos\phi_1 - u)}{\cos\phi_1 - U_2\cos\phi_2} + \frac{u - U_2\cos\phi_2}{\cos\phi_1 - U_2\cos\phi_2}, \tag{2.23}$$

which in terms of the velocity $\tilde{u}$ takes the simpler form

$$T = \tfrac{1}{2}M^2(\gamma-1)[(1+\tilde{U}_2)\tilde{u} - \tilde{u}^2 - \tilde{U}_2] + \frac{T_2(1-\tilde{u})}{1-\tilde{U}_2} + \frac{\tilde{u}-\tilde{U}_2}{1-\tilde{U}_2}. \tag{2.24}$$

Thus, an appropriate transformation reduces the three-dimensional mean flow to a two-dimensional flow with the same Reynolds number, Mach number and temperature ratio, but different velocity ratio $\tilde{U}_2$, plus a uniform flow (U_0, W_0) satisfying (2.15).

Since a skewed mixing layer is equivalent to the sum of a uniform flow and a plane shear flow, the effective convective Mach number for the skewed mixing layer can be

defined as the convective Mach number of the plane shear flow component. The definition of a convective Mach number which is frequently used for a plane mixing layer is (for $\gamma_1 = \gamma_2$)

$$\tilde{M}_c = \frac{1-\tilde{U}_2}{a_1+a_2} = \frac{(1-2U_2\cos\phi+U_2^2)^{\frac{1}{2}}}{1+T_2^{\frac{1}{2}}}M, \tag{2.25}$$

where a_1 and a_2 are the sound speeds of the fast- and slow-moving streams, respectively. This definition was used to collapse the available growth rate data from experiments (Bogdanoff 1983; Papamoschou & Roshko 1988; also see Dimotakis 1991 for a review). Sandham & Reynolds (1990) also use this definition to rescale their linear stability results. This effective convective Mach number plays an important role in studying the compressibility effect on mixing layers.

3. Linear inviscid stability problem

In the linear stability analysis, we perturb the flow field with small wave disturbances in the velocity, temperature, density and pressure with amplitudes which are functions of y. For example, variable f can be decomposed as

$$f = \bar{f} + \mathrm{Re}\{\hat{f}(y)\exp[\mathrm{i}(\alpha x+\beta z-\omega t)]\}, \tag{3.1}$$

where $\bar{f}$ is the mean value, $\hat{f}$ the amplitude of the disturbance, ω the frequency and α and β the wavenumbers in the streamwise (x) and spanwise (z) directions, respectively.

The magnitude of the real part of the wavenumber k_r and the propagation angle θ are given by

$$k_r^2 = \alpha_r^2+\beta_r^2, \quad \tan\theta = \beta_r/\alpha_r, \tag{3.2}$$

where the subscript r denotes the real part of a complex number. For the temporal stability problem, disturbances grow in time and not in space so α and β are real and ω complex with ω_i the temporal amplification rate, where the subscript i denotes the imaginary part. In the spatial problem, disturbances grow in space and not in time, so ω is real and both α and β are complex for a general perturbation such as that evolving from a localized initial disturbance. In this paper, however, we assume that the disturbance is periodic in the z-direction, which is a homogeneous direction for the mean flow, so the disturbance does not amplify for $z\to\pm\infty$, or $\beta_i = 0$. Therefore, the spatial amplification rate is $-\alpha_i$, and if $-\alpha_i > 0$ and Briggs' criteria on amplifying waves (Briggs 1964) is satisfied, then the disturbance is spatially unstable.

Substituting (3.1) into the linearized Euler equations yields the ordinary differential equations for the perturbation amplitudes $\tilde{p}$ and $\hat{v}$:

$$\frac{\mathrm{d}\tilde{p}}{\mathrm{d}y} = -\frac{\mathrm{i}(\alpha u+\beta w-\omega)}{T}\hat{v}, \tag{3.3a}$$

$$\frac{\mathrm{d}\hat{v}}{\mathrm{d}y} = \frac{\mathrm{i}g}{\alpha u+\beta w-\omega}\tilde{p}+\frac{\alpha(\mathrm{d}u/\mathrm{d}y)+\beta(\mathrm{d}w/\mathrm{d}y)}{\alpha u+\beta w-\omega}\hat{v}, \tag{3.3b}$$

where

$$g = (\alpha^2+\beta^2)T - M^2(\alpha u+\beta w-\omega)^2, \tag{3.4}$$

and

$$\tilde{p} = \hat{p}^*/\rho_1^* U_1^{*2} \tag{3.5}$$

is a dimensionless pressure disturbance. When $M \neq 0$ it follows that

$$\tilde{p} = \hat{p}/\gamma M^2, \tag{3.6}$$

and the incompressible limit $M\to 0$ is naturally obtained from (3.3).

Following Gropengiesser (1970), we define a new variable χ:

$$\chi = \mathrm{i}\tilde{p}/\hat{v}, \tag{3.7}$$

which satisfies
$$\frac{\mathrm{d}\chi}{\mathrm{d}y} = \frac{\alpha u+\beta w-\omega}{T} - \frac{g\chi+\alpha(\mathrm{d}u/\mathrm{d}y)+\beta(\mathrm{d}w/\mathrm{d}y)}{\alpha u+\beta w-\omega}\chi, \tag{3.8}$$

and whose boundary conditions are

$$\chi(\pm\infty) = \mp\left[\frac{\alpha u+\beta w-\omega}{(gT)^{\frac{1}{2}}}\right]_{\pm\infty}. \tag{3.9}$$

Substituting the equivalent two-dimensional mean flow (2.12) and (2.15) into the above equations yields

$$\frac{\mathrm{d}\chi}{\mathrm{d}y} = \frac{\tilde{\alpha}\tilde{u}-\tilde{\omega}}{T} - \frac{g\chi+\tilde{\alpha}(\mathrm{d}\tilde{u}/\mathrm{d}y)}{\tilde{\alpha}\tilde{u}-\tilde{\omega}}\chi, \tag{3.10a}$$

$$g = (\tilde{\alpha}^2+\tilde{\beta}^2)\,T - M^2(\tilde{\alpha}\tilde{u}-\tilde{\omega})^2, \tag{3.10b}$$

$$\chi(\pm\infty) = \mp\left[\frac{\tilde{\alpha}\tilde{u}-\tilde{\omega}}{(gT)^{\frac{1}{2}}}\right]_{\pm\infty}, \tag{3.10c}$$

and
$$\tilde{\alpha} = \alpha\cos\psi+\beta\sin\psi, \tag{3.11a}$$

$$\tilde{\beta} = -\alpha\sin\psi+\beta\cos\psi, \tag{3.11b}$$

$$\tilde{\omega} = \omega-\alpha(\cos\phi_1-\cos\psi)-\beta(\sin\phi_1-\sin\psi), \tag{3.11c}$$

where $\tilde{\omega}$ is the Doppler-shifted frequency and $\tilde{\alpha}$ and $\tilde{\beta}$ are the wavenumber components in the directions parallel and normal to $\tilde{u}$, respectively. Since $\tilde{\omega}_i$ may not be zero, the spatial problem for a skewed mixing layer does not reduce to that of an unskewed mixing layer. Similarly, the magnitude of the real part of the wavenumber $\tilde{k}_r$ and the propagation angle $\tilde{\theta}$ are given by

$$\tilde{k}_r^2 = \tilde{\alpha}_r^2+\tilde{\beta}_r^2, \quad \tan\tilde{\theta} = \tilde{\beta}_r/\tilde{\alpha}_r, \tag{3.12}$$

which satisfy
$$\tilde{k}_r = k_r, \quad \tilde{\theta} = \theta+\psi. \tag{3.13}$$

The complex first-order ordinary differential equation (3.8) is subject to two real restrictions from the boundary conditions (3.9). For the temporal problem, α and β are real and ω is complex, so there is a total of four real numbers, leaving two degrees of freedom, which may be chosen as the magnitude of the wavenumber k_r and the propagation angle θ. Also note that the three-dimensional temporal problem reduces to an equivalent unskewed problem.

In a general spatial problem, where ω is real and both α and β are complex, there are five real numbers and thus three degrees of freedom, which may be chosen as the frequency ω_r, the propagation angle θ and the amplification angle $\tan^{-1}(\beta_i/\alpha_i)$. Grosch & Jackson (1991) chose the amplification angle to be the same as θ. In this paper, however, since the z-direction is homogeneous, we assume that the growth is only in the x-direction, i.e. $\beta_i = 0$.

If $(\chi, \alpha, \beta, \omega)$ satisfies the eigenvalue problem (3.8) so does $(-\chi^*, -\alpha^*, -\beta^*, -\omega^*)$, where now the asterisk represents the complex conjugate. This allows ω to be restricted to positive real values in the spatial stability problem.

The stability equations are solved using the numerical scheme (shooting method) described in Sandham & Reynolds (1989). Using the converged eigenvalues found from (3.8), the eigenfunctions are calculated by integrating the linear equations (3.3) from the centreline into the free streams. Initial conditions are calculated from the solution for $\chi(0)$. Therefore, (3.3) can be used to solve the eigenfunctions for both compressible and incompressible flows.

4. Scaling of skewing effect

To isolate the effect of skewing, the linear stability results of the skewed mixing layer are compared with the corresponding results for the unskewed mixing layer with the same free-stream velocity magnitudes and temperatures. From both experiments (e.g. Abramowich 1963; Sabin 1965; Brown & Roshko 1971, 1974; Brown 1974; Papamoschou & Roshko 1988) and linear stability analysis (e.g. Monkewitz & Huerre 1982), it was found that the growth rate of a plane mixing layer can be estimated by using simple combinations of the free-stream quantities (see Dimotakis 1991 for a review). In this section, similar parameters are defined that can be used to scale the growth rate of the skewed mixing layer.

For incompressible plane mixing layers, the convection velocity U_c can be estimated by (see Dimotakis 1986 for details)

$$U_c = \frac{T_2^{\frac{1}{2}} + U_2}{T_2^{\frac{1}{2}} + 1}, \tag{4.1}$$

and the growth rate of a plane mixing layer can be estimated by the ratio of the velocity difference ΔU to the convection velocity U_c

$$\lambda = \frac{\Delta U}{U_c} = \frac{(1-U_2)(T_2^{\frac{1}{2}}+1)}{T_2^{\frac{1}{2}} + U_2}. \tag{4.2}$$

For the skewed incompressible mixing layer, it is reasonable to define a similar effective velocity ratio. The (x, z) components of convection velocity (U_{c_x}, U_{c_z}) can be estimated as

$$U_{c_x} = \frac{T_2^{\frac{1}{2}} \cos\phi_1 + U_2 \cos\phi_2}{T_2^{\frac{1}{2}} + 1}, \tag{4.3a}$$

$$U_{c_z} = \frac{T_2^{\frac{1}{2}} \sin\phi_1 + U_2 \sin\phi_2}{T_2^{\frac{1}{2}} + 1}, \tag{4.3b}$$

where the x-direction is the growth direction. The velocity difference is that of the effective shear, i.e. shear due to the two-dimensional mixing-layer component of the mean flow

$$\Delta U = (1 - 2U_2 \cos\phi + U_2^2)^{\frac{1}{2}}. \tag{4.4}$$

Since the z-direction is assumed to be homogeneous, the skewed mixing layer spatially grows along the x-direction. Therefore, only the x-component convection velocity U_{c_x} affects the spatial growth rate of the mixing layer, and the effective velocity ratio can be defined as

$$\lambda = \frac{\Delta U}{U_{c_x}} = \frac{(1 - 2U_2 \cos\phi + U_2^2)^{\frac{1}{2}}(T_2^{\frac{1}{2}}+1)}{T_2^{\frac{1}{2}} \cos\phi_1 + U_2 \cos\phi_2}, \tag{4.5}$$

which increases with the skewing angle ϕ. Later, this ratio is compared with the normalized linear stability results of the incompressible skewed mixing layer.

For compressible plane mixing layers, Papamoschou & Roshko (1988) found that the growth rate is well represented as a function of only the convective Mach number, when it is normalized by the corresponding growth rate of the incompressible mixing layer with the same velocity and temperature ratios. Linear stability analysis (Ragab & Wu 1988; Sandham & Reynolds 1989) shows this to hold for the maximum amplification rate normalized by that of the corresponding incompressible mixing

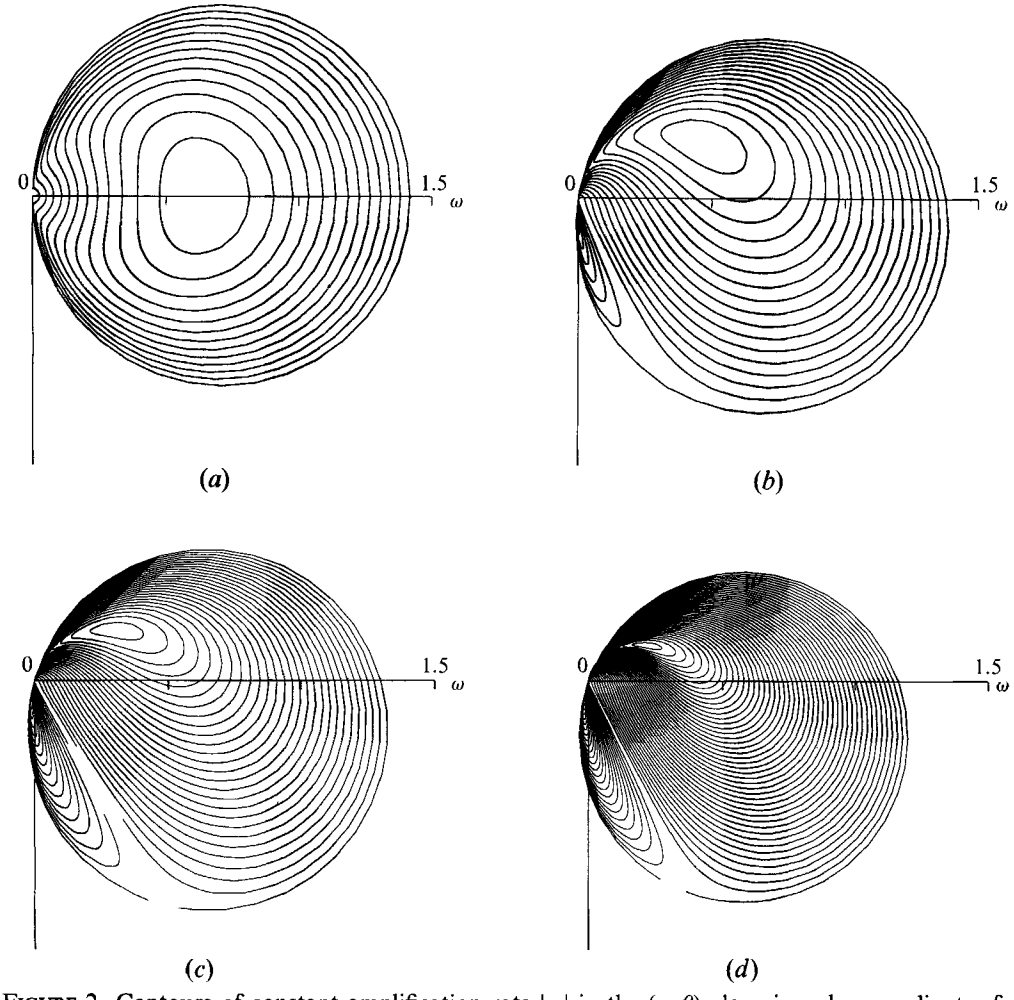

FIGURE 2. Contours of constant amplification rate $|\alpha_i|$ in the (ω, θ)-plane in polar coordinates for incompressible mixing layers with $U_2 = 0.5$, $T_2 = 1$: (*a*) $\phi = 0°$ ($|\alpha_i|_{max} = 0.128$), (*b*) $\phi = 30°$ ($|\alpha_i|_{max} = 0.166$), (*c*) $\phi = 60°$ ($|\alpha_i|_{max} = 0.267$), (*d*) $\phi = 90°$ ($|\alpha_i|_{max} = 0.445$). (The angular coordinate θ is measured from the ω-axis and increases in the clockwise direction. Contour increment for all plots is 0.01 and the outermost contour is neutrally stable.)

layer. For the skewed compressible mixing layer, we have defined the effective convective Mach number $\tilde{M}_c$ in (2.25) and expect that the effective convective Mach number is also the only parameter to describe the intrinsic compressibility effect on the skewed mixing layer. Therefore, the effective velocity ratio λ defined in (4.5) and the effective convective mach number $\tilde{M}_c$ defined in (2.25) together can give an overall estimation of the growth of a skewed compressible mixing layer.

4.1. *Results and scaling of incompressible skewed mixing layers*

For the results in this section, $\phi_1 = 0°$. At zero Mach number, the compressibility effects are absent: from the above discussion that the effective velocity ratio increases with the skewing angle, relative skewing of the two streams is expected to increase the maximum amplification rate.

For the spatial stability problem, since $\beta_1 = 0$, there are two independent parameters which are chosen to be the frequency ω and the propagation angle θ. To study the

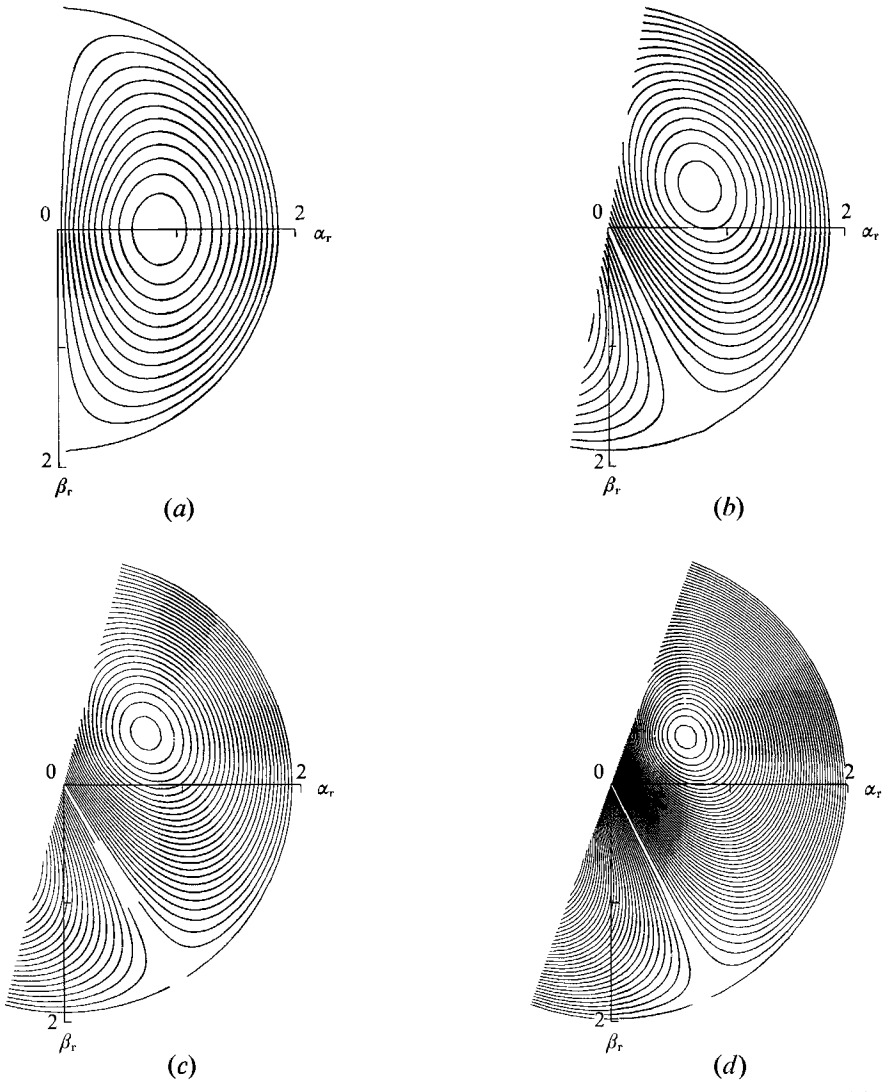

FIGURE 3. Contours of constant amplification rate $|\alpha_i|$ in the wavenumber plane. (Conditions and legend same as figure 2.)

overall skewing effect on the incompressible mixing layer, we show contours of constant spatial amplification rate $-\alpha_i$ in the (ω, θ)-plane in polar coordinates and in the wavenumber (α_r, β_r)-plane in figures 2 and 3, respectively. Contours of constant ω, also in the wavenumber plane, are shown in figure 4. For all plots: $U_2 = 0.5$, $T_2 = 1$, and $\phi = 0°$, 30°, 60° and 90°. Important features of these figures will now be discussed.

Lees & Lin (1946) showed that if a subsonic regular neutral mode exists in the compressible plane mixing layer, its phase velocity must equal the mean velocity at a point where

$$\frac{\mathrm{d}}{\mathrm{d}y}\left(\bar{\rho}\frac{\mathrm{d}\bar{u}}{\mathrm{d}y}\right) = 0. \tag{4.6}$$

Using this result, if $M = 0$, i.e. for incompressible mixing layer, we can show that the wavenumber magnitude of the regular neutral mode is constant for different propagation angles, i.e. the unstable spatial wave are within a half-circle in the

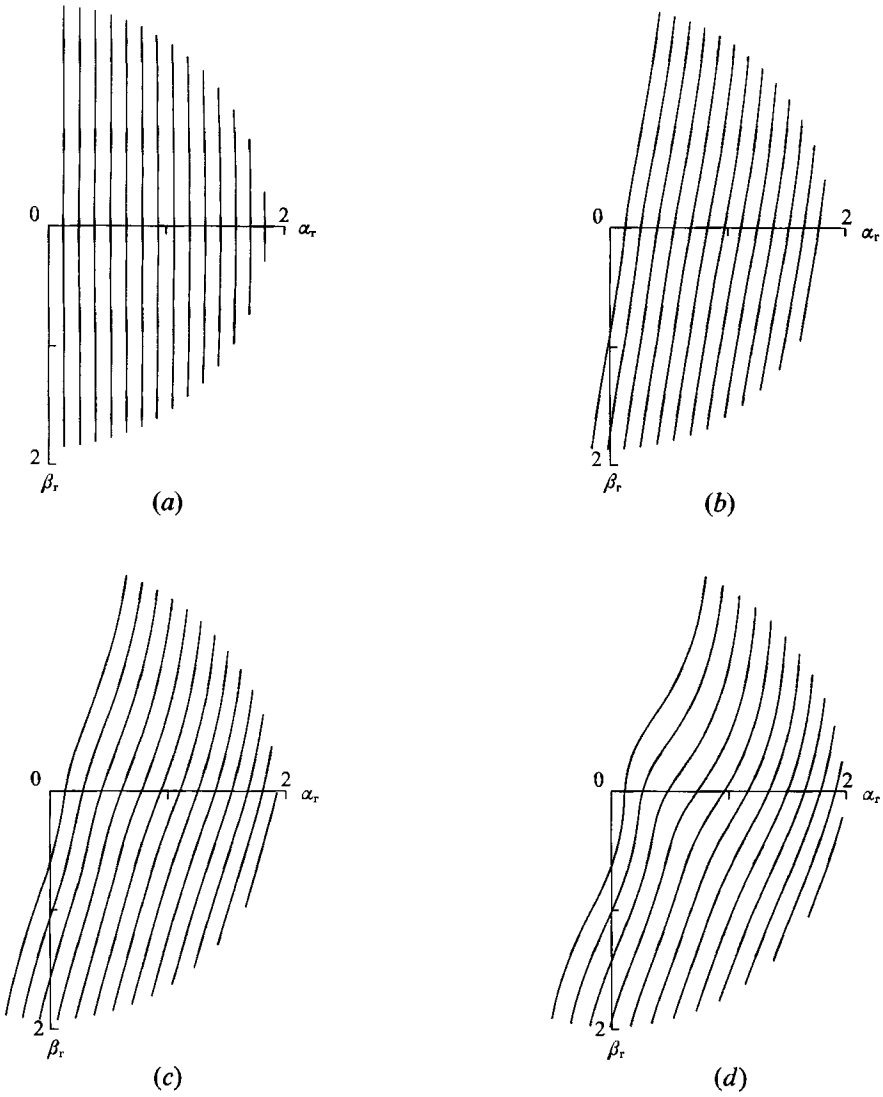

FIGURE 4. Contours of constant frequency ω in the wavenumber plane. (Conditions same as figure 2, contour increment for all plots is 0.1 and the contour closest to origin is 0.1.)

wavenumber plane, which is evident in figures 3 and 4. Since α, β and ω are all real for the neutral mode, Squire's transformation (Drazin & Reid 1981) can be used to show that the regular neutral mode lies on a circle in the (ω, θ)-plane as evident in figure 2.

The laminar mean flow of a skewed mixing layer reduces to an unskewed mixing layer plus a uniform flow, which results in no shear in a special direction. The amplification rate of the wave which travels in this direction is zero. Figures 2 and 3 clearly show this special direction.

In figure 2(*a*), when $\phi = 0°$, the contours are symmetric about $\theta = 0°$, and the most unstable wave is two-dimensional. For $\phi \neq 0°$, the contours are not symmetric, and an oblique wave, whose propagation angle θ is close to ψ, becomes the most amplified wave, i.e. the most unstable wave propagates in approximately the same direction as the effective shear. As skewing increases, the angle of the most amplified wave deviates from ψ as shown in figure 5.

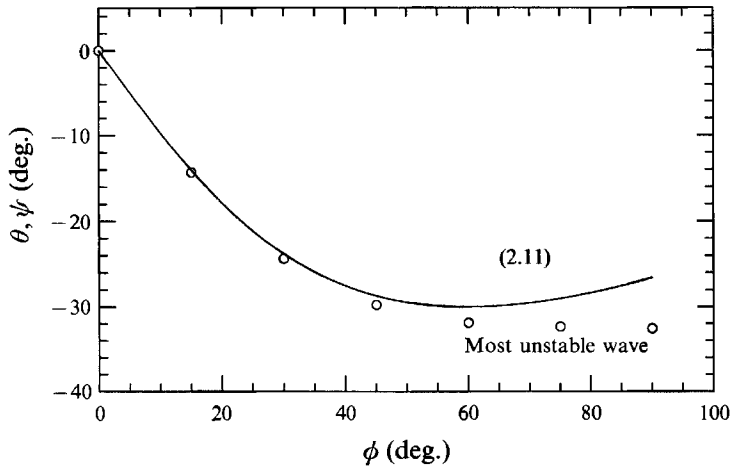

FIGURE 5. Comparison of propagation angle of the most unstable wave with angle of the effective shear as a function of skewing angle for incompressible mixing layers with $U_2 = 0.5$ and $T_2 = 1$.

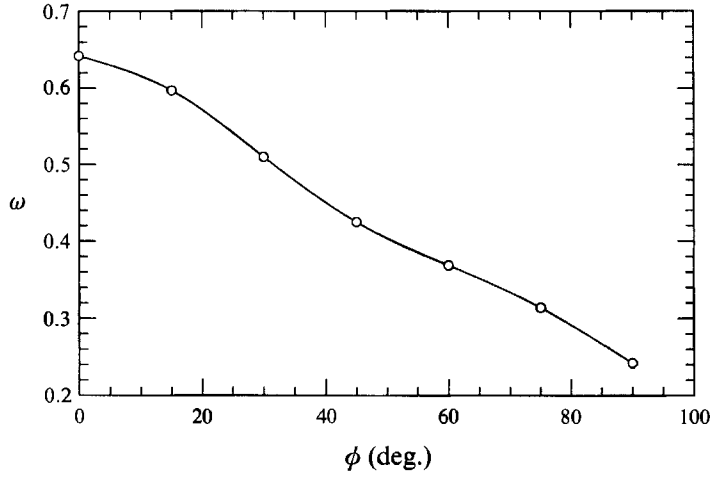

FIGURE 6. Frequency of the most unstable wave as a function of skewing angle for incompressible mixing layers with $U_2 = 0.5$ and $T_2 = 1$.

In figure 4(*a*), when the mixing layer is unskewed, the contours of constant frequency are almost straight lines parallel to the β_r-axis in the wavenumber plane, and the distance between these parallel lines is approximately constant, i.e. the disturbance wave is almost non-dispersive, and the group velocity, which can be defined as the gradient of these contours, is constant and close to the convection velocity. As the skewing angle increases, the angle between the contours and the β_r-axis increases. The direction of the group velocity changes in the same way as the direction of the convection velocity defined in (4.3). With large skewing, the contours in figures 4(*c*, *d*) are no longer straight lines, i.e. the disturbance wave becomes dispersive.

Figure 4 shows that the lines of constant frequency rotate clockwise as skewing increases, while figure 5 shows that the propagation angle of the most unstable wave decreases. These two opposite rotations make the frequency of the most unstable wave decrease with the skewing angle, shown in figure 6. However, the wavenumber magnitude of the most amplified wave does not decrease that much (figure 3).

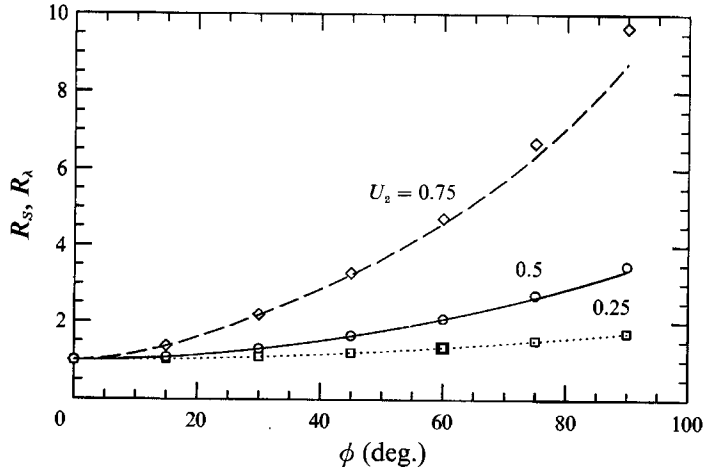

FIGURE 7. Comparison of normalized maximum amplification rate R_S with normalized effective velocity ratio R_λ as a function of skewing angle for incompressible mixing layers with $T_2 = 1$ and $U_2 = 0.25$, 0.5 and 0.75 (Symbols denote R_S and lines denote R_λ.)

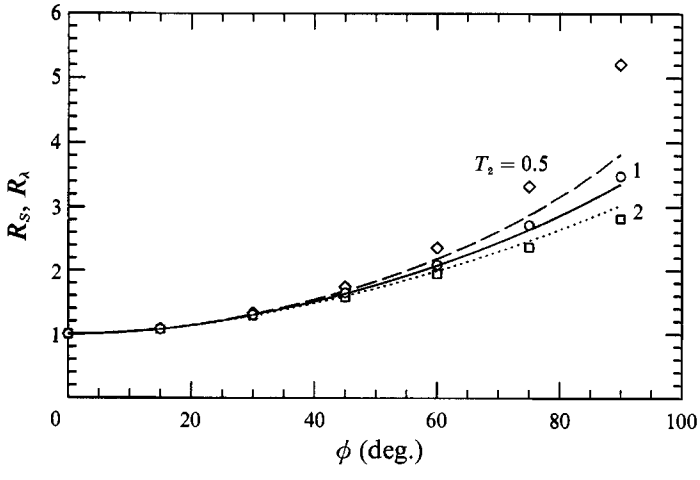

FIGURE 8. Comparison of normalized maximum amplification rate R_S with normalized effective velocity ratio R_λ as a function of skewing angle for incompressible mixing layers with $U_2 = 0.5$ and $T_2 = 0.5$, 1 and 2 (Symbols denote R_S and lines denote R_λ.)

The contour increments for all plots in figure 2 are the same, and it is clear that the maximum amplification rate increases with ϕ. To isolate this skewing effect on the amplification rate, we normalize the maximum amplification rate using the corresponding value of an unskewed mixing layer with the same velocity ratio and temperature ratio. This normalized maximum amplification rate is defined as

$$R_S = \frac{|\alpha_i|_{\max}(U_2, T_2, \phi)}{|\alpha_i|_{\max}(U_2, T_2, 0)}. \tag{4.7}$$

Figure 7 shows the normalized maximum amplification rate R_S as a function of the skewing angle ϕ for uniform temperature (density), and velocity ratios $U_2 = 0.25$, 0.5

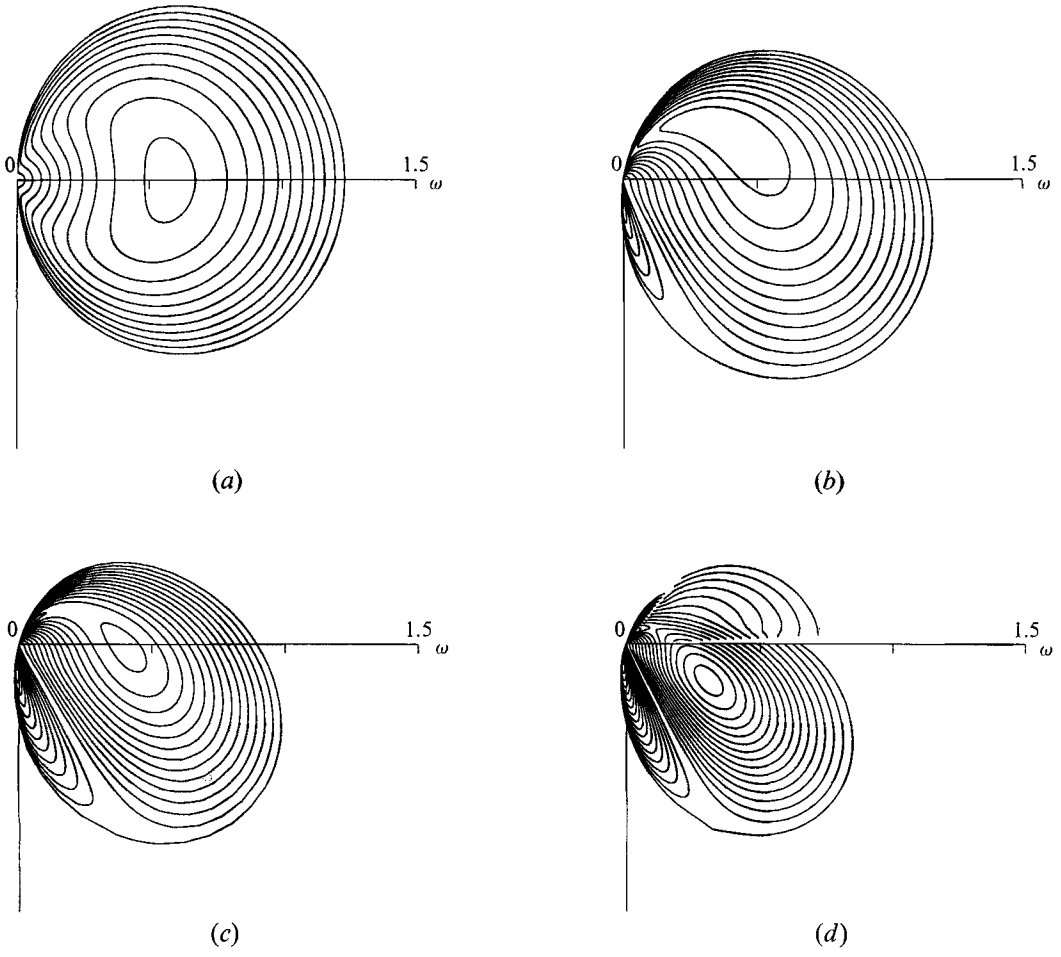

FIGURE 9. Contours of constant amplification rate $|\alpha_i|$ in the (ω, θ)-plane in polar coordinates for compressible mixing layers with $M = 1.6$, $U_2 = 0.5$, $T_2 = 1$: (*a*) $\phi = 0°$ ($|\alpha_i|_{max} = 0.103$), (*b*) $\phi = 30°$ ($|\alpha_i|_{max} = 0.117$), (*c*) $\phi = 60°$ ($|\alpha_i|_{max} = 0.135$), (*d*) $\phi = 90°$ ($|\alpha_i|_{max} = 0.172$). (The angular coordinate θ is measured from the ω-axis and increases in the clockwise direction. Contour increment for all plots is 0.01 and the outermost contour is neutrally stable.)

and 0.75. The maximum amplification rate increases with the skewing angle, and the skewing effect increases with the velocity ratio U_2. We also show in the same plot the normalized effective velocity ratio R_λ, normalized in the same way as (4.7), which agrees very well with the maximum amplification rate. The increase in the maximum amplification rate with skewing can thus be estimated from the increase in the effective velocity ratio.

To examine if this scaling also holds for $T_2 \neq 1$, the normalized maximum amplification rates for $U_2 = 0.5$ and $T_2 = 0.5$, 1 and 2 are shown in figure 8. When the skewing angle is not very large, the influence of temperature (density) ratio is small and the maximum amplification rate is reasonably predicted by the effective velocity ratio scaling. For skewing angles ϕ larger than 60°, the skewing effect increases with decreasing temperature ratio T_2, and the maximum amplification rate does not agree well with the effective velocity ratio. One reason for this may be the deviation of the propagation direction of the most unstable wave from the effective shear direction as

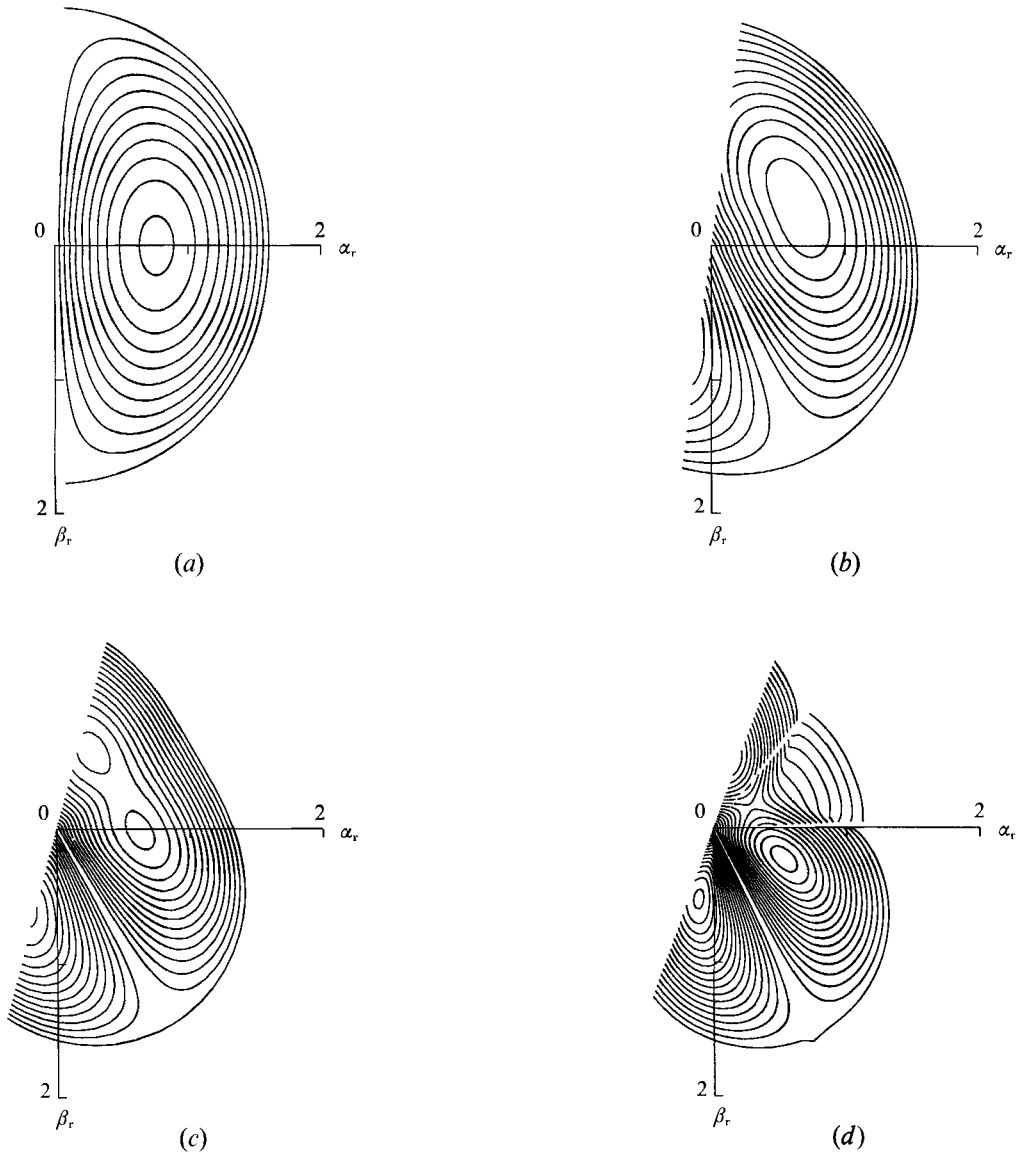

FIGURE 10. Contours of constant amplification rate $|\alpha_i|$ in the wavenumber plane. (Conditions and legend same as figure 9.)

shown in figure 5. Also recall that waves become dispersive when skewing is large. Another reason may be that the convection velocity in (4.3) is not accurate when T_2 is not very close to one (Dimotakis 1986).

4.2. *Results and scaling of compressible skewed mixing layers*

For compressible mixing layers, skewing increases the effective convective Mach number $\tilde{M}_c$ as well as the effective velocity ratio λ. Since compressibility stabilizes the mixing layer, the skewing effect on the amplification rate is expected to decrease.

Figures 9 and 10 show contours of constant amplification rate $-\alpha_i$ in the (ω, θ)-plane in polar coordinates and in the wavenumber (α_r, β_r)-plane, respectively. Figure

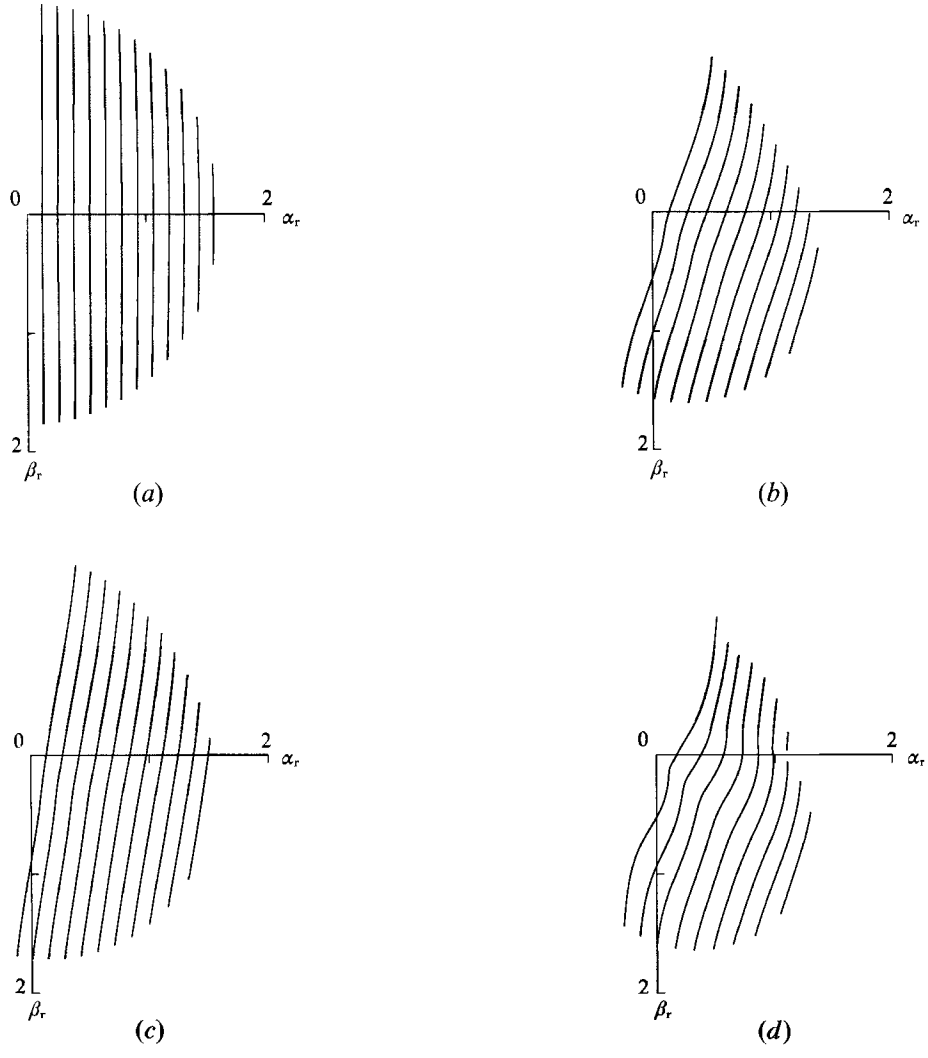

FIGURE 11. Contours of constant frequency ω in the wavenumber plane. (Conditions same as figure 9, contour increment for all plots is 0.1 and the contour closest to origin is 0.1.)

11 shows contours of constant frequency ω in the wavenumber plane. For all plots: $M = 1.6$, $U_2 = 0.5$, $T_2 = 1$, and $\phi = 0°$, 30°, 60° and 90°.

In figure 9(*a*), $\phi = 0°$ and $M_c = 0.4$. At this Mach number, the compressibility effect is not significant, and the behaviour is quite similar to that of the incompressible mixing layer shown in figure 2(*a*), although the peak amplification rate is less than that of the corresponding incompressible mixing layer. As the two free-streams are skewed, the effective velocity ratio increases, which tends to increase the maximum amplification rate. However, the effective convective Mach number, and thus the compressibility effect, also increases, tending to reduce the maximum amplification rate. As will be shown later (figure 15), the net effect of skewing is to increase the maximum amplification rate.

It was found (Gropengiesser 1970; Jackson & Grosch 1989; Sandham & Reynolds 1989) that for compressible plane mixing layers, the most unstable waves become two symmetric oblique waves when the convective Mach number is larger than some

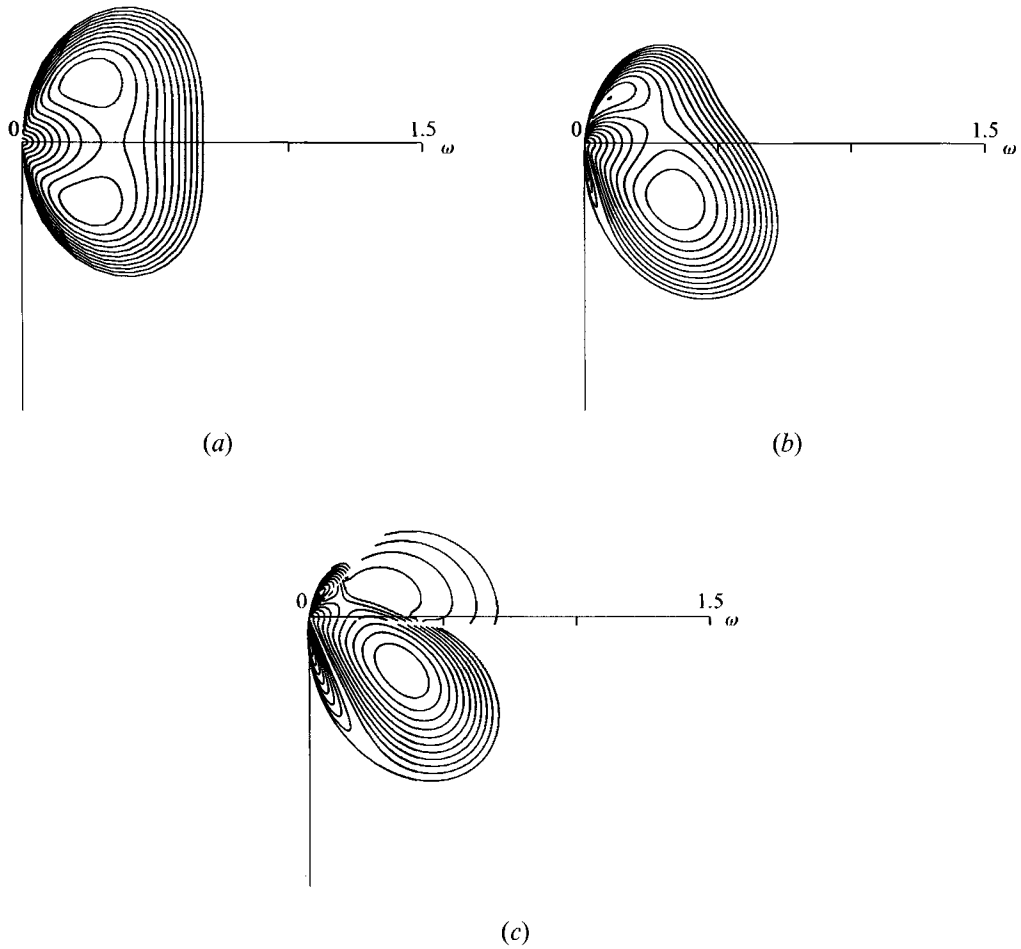

FIGURE 12. Contours of constant amplification rate $|\alpha_i|$ in the (ω, θ)-plane in polar coordinates for compressible mixing layers with $M = 3.2$, $U_2 = 0.5$, $T_2 = 1$: (*a*) $\phi = 0°$ ($|\alpha_i|_{max} = 0.0557$), (*b*) $\phi = 15°$ ($|\alpha_i|_{max} = 0.0560$), (*c*) $\phi = 30°$ ($|\alpha_i|_{max} = 0.0558$). (The angular coordinate θ is measured from the ω-axis and increases in the clockwise direction. Contour increment for all plots is 0.005 and the outermost contour is neutrally stable.)

critical value. Sandham & Reynolds (1989) further proposed an empirical relation for the angle of the most amplified disturbance as

$$M_c \cos\theta \approx 0.6. \tag{4.8}$$

However, for the skewed compressible mixing layers in figure 10(*c*) ($\phi = 60°$ and $\tilde{M}_c = 0.69$), there are two maxima of the amplification rate, which are not symmetric and whose values are not exactly the same. The positions of the two maxima in the wavenumber plane are also very different from the plane mixing layer.

Similar to the incompressible mixing layer, the amplification rate of the wave which propagates in the direction perpendicular to the effective shear is zero as shown in figures 9 and 10. In figure 11, the frequency contours are straight lines and parallel to each other for small skewing angles, and the instability waves become dispersive for large skewing angles.

As the Mach number is increased, the compressibility effect increases. To illustrate this change, we show contours of constant amplification rate $-\alpha_i$ in the (ω, θ)-plane

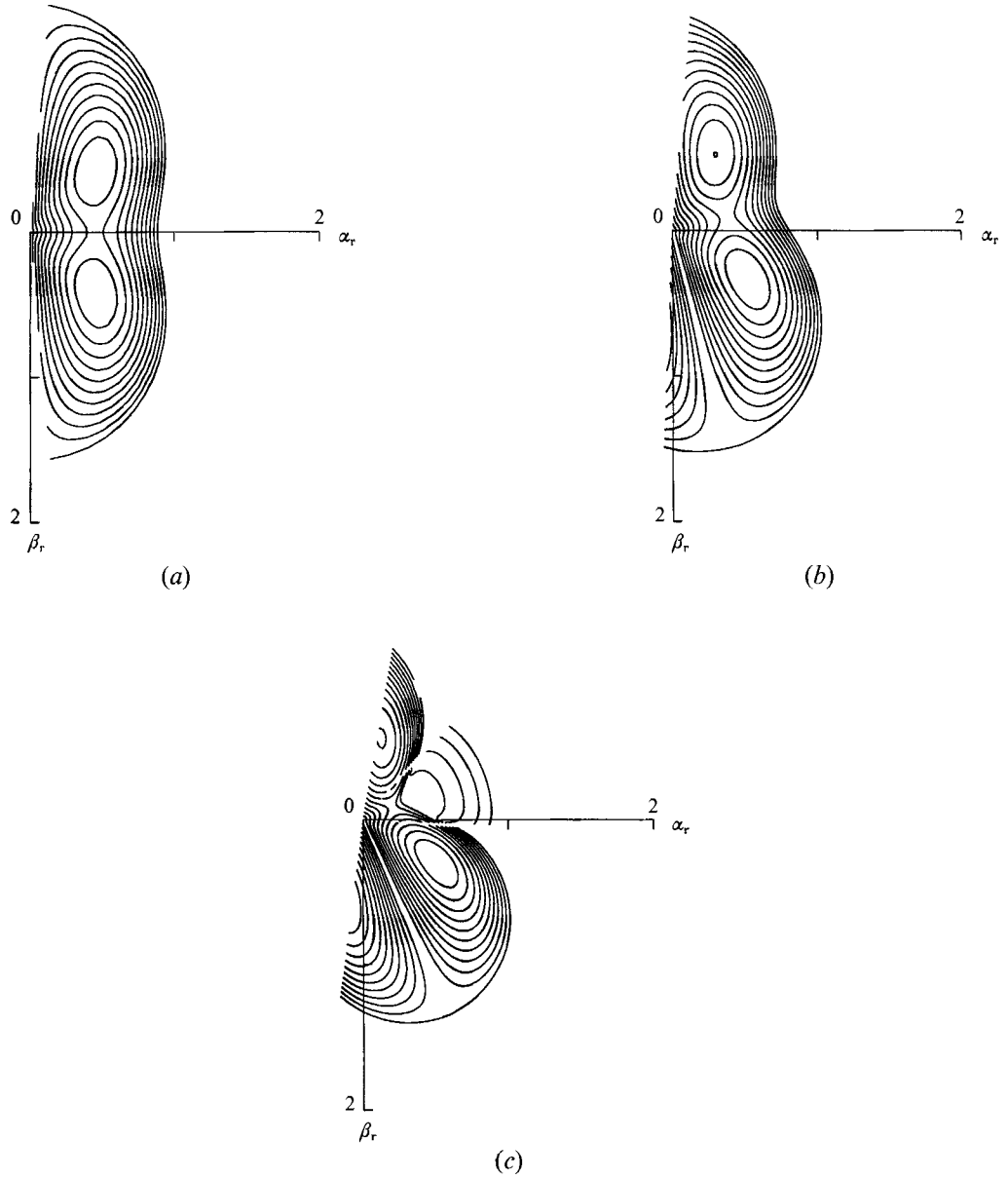

FIGURE 13. Contours of constant amplification rate $|\alpha_i|$ in the wavenumber plane. (Conditions and legend same as figure 12.)

and the wavenumber plane in figures 12 and 13, respectively, and contours of constant frequency ω in the wavenumber plane in figure 14 for $M = 3.2$, $U_2 = 0.5$, $T_2 = 1$ and $\phi = 0°$, 15° and 30°. In figure 12(*a*), $\phi = 0°$ and $M_c = 0.8$. At this convective Mach number, two symmetric oblique waves ($\theta \approx \pm 43°$) are the most unstable waves, and their amplification rate is much less than that of the corresponding incompressible mixing layer. In figure 14, as the skewing angle ϕ increases, to keep with the direction of the convection velocity, the lines of constant frequency rotate clockwise, and the pattern of the constant amplification rate in figure 13 rotates counterclockwise to follow the direction of the effective shear. In figure 12(*b*, *c*) the frequency of the most

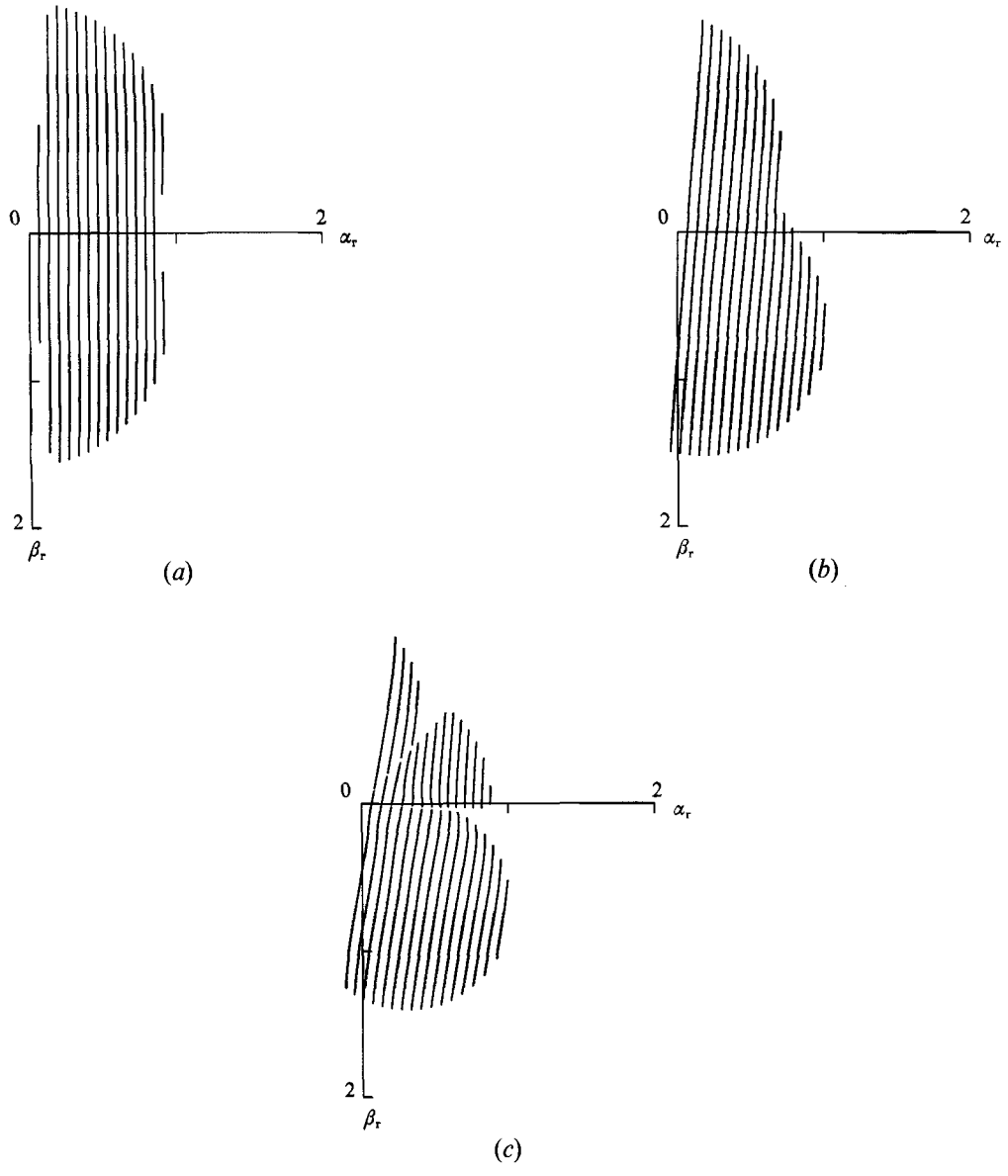

FIGURE 14. Contours of constant frequency ω in the wavenumber plane. (Conditions same as figure 12, contour increment for all plots is 0.05 and the contour closest to origin is 0.05.)

unstable wave in the upper quadrant becomes smaller. In the (ω, θ)-plane, the upper pattern is squeezed down, while the lower pattern is stretched.

Previous researchers (Lessen, Fox & Zien 1965, 1966; Gropengiesser 1970; Jackson & Grosch 1989) have found other instability modes at high convective Mach number for the plane mixing layer. Jackson & Grosch (1989) classified these modes as a fast supersonic mode (supersonic relative to the low-speed stream) and a slow supersonic mode (supersonic relative to the high-speed stream). These supersonic modes also occur in the skewed mixing layer (Grosch & Jackson 1991). Figure 12(*c*) ($\phi = 30$, $\tilde{M}_c = 0.99$) shows the supersonic mode, but the most unstable wave happens to be a subsonic mode.

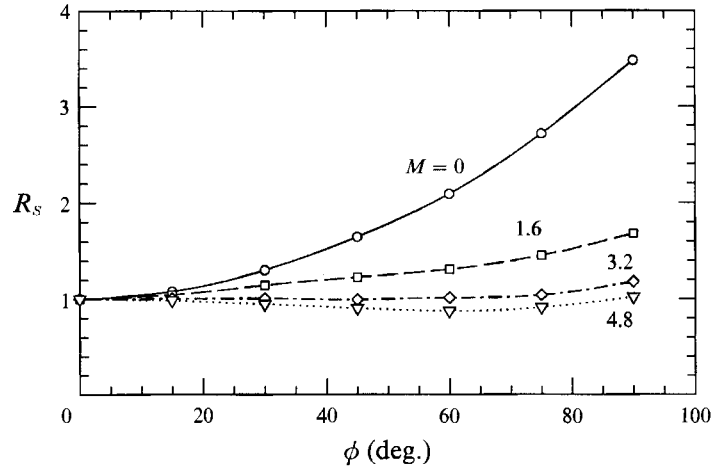

FIGURE 15. Normalized maximum amplification rate R_S as a function of skewing angle for different Mach number; $U_2 = 0.5$, $T_2 = 1$.

Figure 15 shows the normalized maximum amplification rate R_S as a function of the skewing angle ϕ for $U_2 = 0.5$, $T_2 = 1$ and $M = 0$, 1.6, 3.2 and 4.8. For medium free-stream Mach number, skewing still increases the maximum amplification rate. When $M = 3.2$, i.e. $M_c = 0.8$ for the unskewed mixing layer, the maximum amplification rate is almost constant with ϕ. When $M > 3.2$, skewing decreases the maximum amplification rate for small ϕ.

To scale this compressibility effect we, instead, normalize the maximum amplification rate of the compressible skewed mixing layer using the results from the corresponding incompressible skewed mixing layer, that is

$$R_C = \frac{|\alpha_i|_{\max}(M, U_2, T_2, \phi)}{|\alpha_i|_{\max}(0, U_2, T_2, \phi)} = R_C(\tilde{M}_c). \tag{4.9}$$

Figure 16 shows the normalized amplification rate R_C of the compressible skewed mixing layer as a function of the effective convective Mach number $\tilde{M}_c$ for $U_2 = 0.5$ and different Mach number M and temperature ratio T_2. All data collapse to the values of the plane compressible mixing layer with $U_2 = 0.5$ and $T_2 = 1$ (shown by the solid line), indicating that the scaling (4.9) is successful. The lack of collapse for temperature ratio $T_2 \neq 1$ may be due to either an inaccuracy in the estimation of convection velocity (4.3) or the fact that $\tilde{M}_c$ is simply a first-order compressibility parameter (Sandham & Reynolds 1990). With this qualification, the compressibility effect on skewed mixing layers can be scaled using only the effective convective Mach number.

Note that ϕ_1 is fixed at 0° in the above discussion; if it is also allowed to vary but ϕ as well as U_2, T_2 and M are fixed, the effective velocity ratio λ in (4.5) can be increased. Since the effective convective Mach number $\tilde{M}_c$ in (2.25) remains constant, further enhancement can still be obtained even for a highly compressible flow.

5. Discussion

In the previous section, we assumed that the amplification in the z-direction is zero. This assumption should be valid if the splitter plate edge is wide enough and dominantly excites the unstable waves. To compare our results with the assumption of

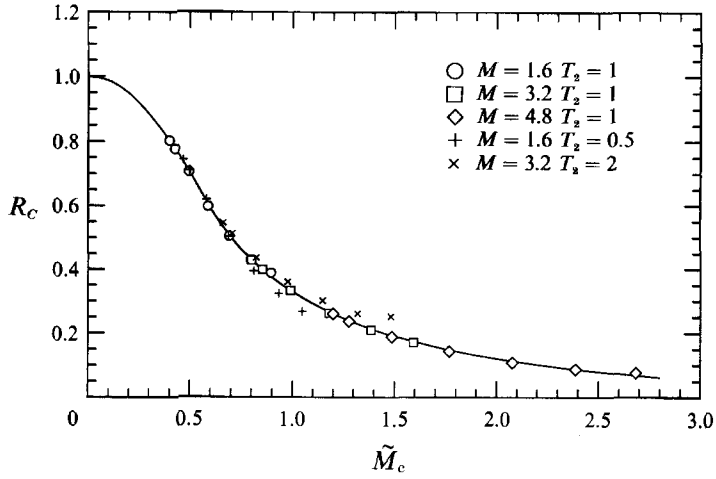

FIGURE 16. Comparison of the normalized maximum amplification rate R_C of skewed mixing layers with that of plane mixing layer as a function of effective convective Mach number $\tilde{M}_c$; $U_2 = 0.5$. (Solid line denotes R_C of plane mixing layers with $T_2 = 1$ and symbols denote R_C of skewed mixing layers.)

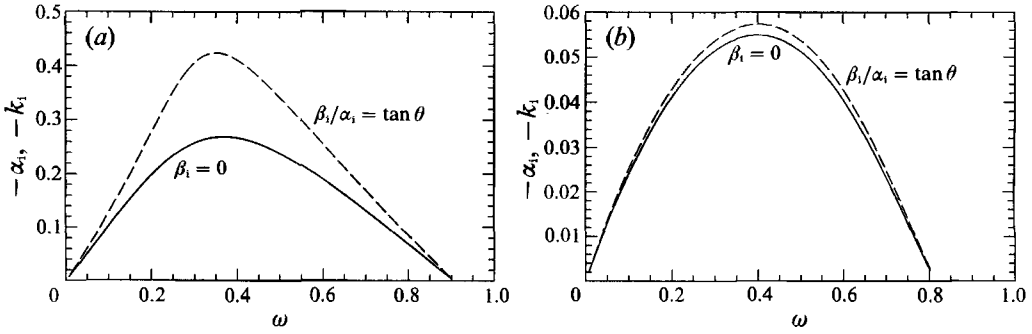

FIGURE 17. Comparison of the amplification rate obtained under the assumptions that the amplification direction is the x-direction or the propagation direction for $U_2 = 0.5$, $T_2 = 1$: (*a*) $M = 0$, $\phi = 60°$ and $\theta = -30°$, (*b*) $M = 3.2$, $\phi = 30°$ and $\theta = 30°$.

Grosch & Jackson (1991) that the amplification direction is the same as the propagation direction, we show the amplification rates obtained under these two assumptions as a function of frequency ω in figure 17 for $U_2 = 0.5$, $T_2 = 1$, and (*a*) $M = 0$, $\phi = 60°$ and $\theta = -30°$; (*b*) $M = 3.2$, $\phi = 30°$ and $\theta = 30°$. The assumption made by Grosch & Jackson can sometimes substantially overestimate the amplification rate. This overestimation can be simply explained by a relation between spatial growth rates along different amplification directions (Nayfeh 1980).

As mentioned before, the only available measurement of skewed mixing layers was conducted by Hackett & Cox (1970). Using our convention, for their two-stream case, $M = 0$, $U_2 = T_2 = 1$, $\phi = -45°$ and $\phi_2 = 45°$ ($\phi = 90°$); for the single-stream case, $M = 0$, $U_2 = 0$, $T_2 = 1$ and $\phi_1 = 45°$ ($\phi = 0$). From (4.5), the effective velocity ratios for the two-stream cases and the single-stream case are $\lambda_b = 2$ and $\lambda_s = 2\sqrt{2}$, respectively. Their ratio is $1/\sqrt{2} = 0.71$. For the single-stream case, Hackett & Cox found that skewing the splitter edge has little effect on the two-dimensional shear layer, which is consistent with our assumption that the direction parallel to the edge is homogeneous

and simple geometric consideration may be used to obtain the growth rate in an arbitrary direction. From their experimental results, the ratio of the spreading rates between the two cases is approximately 0.70, which is very close to our estimation.

It was found that for a plane mixing layer, the maximum amplification rate of the linear stability analysis can predict the spreading rate of the turbulent mixing layer observed in experiments (Dimotakis 1991). Since the effective velocity ratio λ agrees very well with the maximum amplification rate, as shown in figure 7, we expect that the effective velocity ratio can be used to predict the amplification rate of the skewed mixing layer. Similarly the collapse of data from different Mach numbers onto a single curve in figure 16 suggests that the compressibility effect can be estimated by using only the effective convective Mach number.

6. Conclusions

The inviscid instability of a skewed mixing layer is studied in this paper. The laminar mean flow in a skewed mixing layer reduces to the sum of a uniform flow and a two-dimensional mixing layer with the same temperature (density) ratio, a different velocity ratio and a different convective Mach number. The temporal stability problem reduces to an equivalent planar temporal problem, but the spatial problem does not reduce to an equivalent planar spatial analogue.

For the spatial stability problem, we define an effective velocity ratio which can be used to estimate the amplification rate of an incompressible skewed mixing layer. Skewing the two free streams can increase the amplification rate of the incompressible mixing layer by a factor of three for $U_2 = 0.5$ and $T_2 = 1$. The enhancement is nine fold for $U_2 = 0.75$ and $T_2 = 1$.

For the compressible skewed mixing layer, we found that the effective convective Mach number can be used to estimate the normalized amplification rate. Skewing increases the amplification rate for the compressible mixing layer with medium convective Mach number ($M_c < 0.8$). However, for very high convective Mach number, skewing decreases the maximum amplification rate.

This work was performed under grant AFOSR-91-0374 monitored by Dr J. McMichael. The computations reported in the paper were performed on the NAS Facility at NASA-Ames. We appreciate helpful comments of Mr S. Scott Collis on a draft of this paper. We also thank the referees for their helpful comments.

REFERENCES

ABRAMOWICH, G. N. 1963 *The Theory of Turbulent Jets*. MIT Press.

BOGDANOFF, D. W. 1983 Compressibility effects in turbulent shear layers. *AIAA J.* **21**, 926–927.

BRIGGS, R. J. 1964 Electron-stream interaction with plasmas. *Research Monograph* 29. MIT Press.

BROWN, G. L. 1974 The entrainment and large structure in turbulent mixing layers. In *Proc. 5th Australian Conf. on Hydraulics and Fluid Mechanics* (ed. D. Lindly & A. J. Sutherland), pp. 352–359. University of Canterbury, Christchurch, New Zealand.

BROWN, G. L. & ROSHKO, A. 1971 The effect of density difference on the turbulent mixing layer. *AGARD-CP*-93, pp. 23-1–23-12.

BROWN, G. L. & ROSHKO, A. 1974 On density effects and large structure in turbulent mixing layers. *J. Fluid Mech.* **64**, 775–816.

DIMOTAKIS, P. E. 1986 Two-dimensional shear-layer entrainment. *AIAA J.* **24**, 1791–1796.

DIMOTAKIS, P. E. 1991 Turbulent free shear layer mixing and combustion. *GALCIT Rep.* FM91-2.

DRAZIN, P. G. & REID, W. H. 1981 *Hydrodynamic Stability*. Cambridge University Press.

GROPENGIESSER, H. 1970 Study on the stability of boundary layers and compressible fluids. *NASA Tech. Transl.* NASA TT F-12, 786.

GROSCH, C. E. & JACKSON, T. L. 1991 Inviscid spatial stability of a three-dimensional compressible mixing layer. *J. Fluid Mech.* **231**, 35–50.

GRÜNDEL, H. & FIEDLER, H. E. 1992 The mixing layer between non-parallel streams. In *Fourth European Turbulence Conf. Abstracts*, pp. 27–29. Delft University of Technology, The Netherlands.

HACKETT, J. E. & COX, D. K. 1970 The three-dimensional mixing layer between two grazing perpendicular streams. *J. Fluid Mech.* **43**, 77–96.

JACKSON, T. L. & GROSCH, C. E. 1989 Inviscid spatial stability of a compressible mixing layer. *J. Fluid Mech.* **208**, 609–637.

LEES, L. & LIN, C. C. 1946 Investigation of the stability of the laminar boundary layer in a compressible fluid. *NACA TN* 1115.

LELE, S. K. 1989 Direct numerical simulation of compressible free shear flows. *AIAA Paper*, 89-0374.

LESSEN, M., FOX, J. A. & ZIEN, H. M. 1965 On the inviscid stability of the laminar mixing of two parallel streams of a compressible fluid. *J. Fluid Mech.* **23**, 355–367.

LESSEN, M., FOX, J. A. & ZIEN, H. M. 1966 Stability of the laminar mixing of two parallel streams with respect to supersonic disturbances. *J. Fluid Mech.* **25**, 737–742.

MACARAEG, M. G. 1991 Investigation of supersonic modes and three-dimensionality in bounded, free shear flows. *Comput. Phys. Commun.* **65**, 201–208.

MONKEWITZ, P. A. & HUERRE, P. 1982 Influence of the velocity ratio on the spatial instability of mixing layers. *Phys. Fluids* **25**, 1137–1143.

NAYFEH, A. H. 1980 Stability of three-dimensional boundary layers. *AIAA J.* **18**, 406–416.

PAPAMOSCHOU, K. & ROSHKO, A. 1988 The compressible turbulent shear layer: an experimental study. *J. Fluid Mech.* **197**, 453–477.

RAGAB, S. A. & WU, J. L. 1988 Instabilities in the free shear layer formed by two supersonic streams. *AIAA Paper* 88-3677.

SABIN, C. M. 1965 An analytical and experimental investigation of the plane, incompressible, turbulent free-shear layer with arbitrary velocity ratio and pressure gradient. *Trans. ASME* D: *J. Basic Engng* **87**, 421–428.

SANDHAM, N. D. & REYNOLDS, W. C. 1989 A numerical investigation of the compressible mixing layer. *Rep.* TF-45. Department of Mechanical Engineering, Stanford University, Stanford, California.

SANDHAM, N. D. & REYNOLDS, W. C. 1990 Compressible mixing layer: linear theory and direct simulation. *AIAA J.* **28**, 618–624.

SCHLICHTING, H. 1979 *Boundary-Layer Theory*, 7th edn. McGraw-Hill.